Made available through Montana State University's ScholarWorks

# Ureolysis-induced calcium carbonate precipitation (UICP) in the presence of CO2-affected brine: a field demonstration

Catherine M. Kirkland, Arda Akyel, Randy Hiebert, Jay McCloskey, Jim Kirksey, Alfred B. Cunningham, Robin Gerlach, Lee Spangler, Adrienne J. Phillips

© This manuscript version is made available under the CC-BY-NC-ND 4.0 license https://creativecommons.org/licenses/by-nc-nd/4.0/

# Ureolysis-induced calcium carbonate precipitation (UICP) in the presence of $CO_2$-affected brine: a field demonstration

Catherine M. Kirkland[1,2*], Arda Akyel[1,3,] Randy Hiebert[4], Jay McCloskey[4], Jim Kirksey[5], Alfred B. Cunningham[1,2], Robin Gerlach[1,3], Lee Spangler[6], and Adrienne J. Phillips[1,2]

[1]Center for Biofilm Engineering, Montana State University, 366 Barnard Hall, Bozeman, MT 59717
[2]Department of Civil Engineering, Montana State University, 205 Cobleigh Hall, Bozeman, MT 59717
[3]Department of Chemical and Biological Engineering, Montana State University, 214 Roberts Hall, Bozeman, MT 59717
[4]Montana Emergent Technologies, 160 W Granite St, Butte, MT 59701
[5]Loudon Technical Services LLC, 1611 Loudon Heights Rd, Charleston, WV, 25314
[6]Energy Research Institute, Montana State University, P.O. Box 172465, Bozeman, MT 59717

## Highlights

- UICP in the presence of $CO_2$-affected brine reduced injectivity in a wellbore cement channel by an order of magnitude.
- Ultrasonic imaging logs conducted after UICP treatment showed additional solids behind the casing which extended at least 30 m (100 ft) above the injection zone.
- Urease enzyme from heat-treated microbial cultures was an effective catalyst for UICP reactions.

## Graphical Abstract

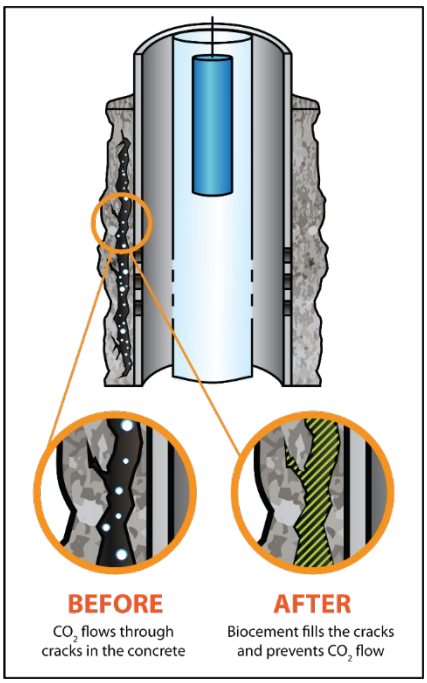

**Abstract**

Biomineralization is an emerging biotechnology for subsurface engineering applications like remediating leaky wellbores. The process relies on ureolysis to induce precipitation of calcium carbonate in undesired flow paths. In geologic storage of $CO_2$, there is a potential for leakage and low pH conditions, thus, ureolysis-induced calcium carbonate precipitation (UICP) was tested at field scale to seal a channel in the wellbore cement annulus in the presence of $CO_2$-affected brine. Conventional oil field methods were used to deliver UICP-promoting fluids downhole to the treatment zone approximately 1000 feet (305 m) below ground surface (bgs). Over 4 days, 242 L (64 gal) of heat-treated *Sporosarcina pasteurii* cultures (22 bailers) and 329 L (87 gal) of urea – calcium chloride solution (30 bailers) were injected. The UICP treatment resulted in a 94% reduction of injectivity and ultrasonic well logging showed a noticeable increase in the percentage of solids in the channel outside the casing, including more than 30 m (100 ft) above the injection point. Subsequent well logging 11 months after the field demonstration showed that a significant portion of the new solids remained but the seal was compromised following sustained pumping. The results of this experiment suggest that UICP can be promoted in the presence of $CO_2$-affected brine to seal leakage pathways. Additional research is required to optimize long term seal integrity to ensure storage of $CO_2$ in geologic carbon sequestration scenarios.

**Keywords**

Ureolysis-induced calcium carbonate precipitation, UICP, wellbore integrity, *Sporosarcina pasteurii*, $CO_2$ sequestration

## 1. Introduction

### *1.1 Background*

Rising levels of $CO_2$ in the atmosphere must be reduced to achieve climate change mitigation goals and limit the projected average global temperature increase [1]. A significant part

of this effort is carbon capture and sequestration (CCS) wherein $CO_2$ captured from point sources like coal-fired power plants or chemical processing facilities is compressed to a supercritical state and injected into subsurface storage reservoirs for sequestration on geologic time scales [2]. Maintaining wellbore integrity is essential to ensuring that sequestered $CO_2$ stays trapped in subsurface reservoirs and is not re-emitted to the atmosphere via leakage pathways in the near wellbore environment. Current state of the art for mitigating leaky wellbores [3] where conventional squeeze cementing is not appropriate includes use of fine cement, resins [4], and nanomaterials [5, 6]. Many of these methods are appropriate for leakage pathways on the order of 100 μm or larger but cannot penetrate micro-scale cracks due to the high viscosity of the sealing agents. Biocement, produced during the process of ureolysis-induced calcium carbonate precipitation (UICP), is emerging as a contender to aid in wellbore sealing applications where more conventional methods are unsuccessful or inappropriate [7-9]. In this study, we report on a field study which applied UICP in the presence of $CO_2$-affected brine to repair compromised cement in a test well.

### *1.2 UICP Fundamentals*

It has long been known that enzyme catalysis can be harnessed to hydrolyze urea and precipitate calcium carbonate [10]. The enzyme urease is widespread in nature and can be found in microbes like bacteria and algae, as well as in fungi and plants [11]. Ureolysis results in a pH increase and produces bicarbonate ($HCO_3^-$) and carbonate ($CO_3^{2-}$) ions. When calcium ($Ca^{2+}$) activity is sufficient to exceed saturation conditions, calcium carbonate ($CaCO_3$) precipitation can occur [Eqn. 1].

$$\mathrm{CO(NH_2)_2} + 2\mathrm{H_2O} + \mathrm{Ca^{2+}} \rightarrow 2\mathrm{NH_4^+} + \mathrm{CaCO_3}\,(s) \qquad [1]$$

During ureolysis-induced calcium carbonate precipitation (UICP), ureolytic bacterial cultures can serve as both the source of the urease enzyme and can form a biofilm matrix on surfaces. Additionally, the biofilm is believed to provide nucleation sites for precipitation to initiate [12-14]. Over multiple injections of ureolytic cultures and UICP-promoting media, the $CaCO_3$ mineral thickens, bridges pore throats and fractures, fills voids, and ultimately seals flow pathways [15].

*1.3 Project overview*

The primary goal of this project was to assess the ability of UICP to form a bio-cement seal in the near wellbore environment in the presence of $CO_2$-affected brine. Dissolved $CO_2$ reduces the brine pH and the fraction of $CO_3^{2-}$ ions in solution, thereby potentially making $CaCO_3$ precipitation less likely and instead favoring dissolution of carbonate minerals. Since UICP has been successful in sealing leaky wellbores in the oil and gas industry [7, 8], it is important to assess the extent to which the process could be applied in the context of $CO_2$ sequestration where exposure to $CO_2$-affected brine is possible.

A secondary goal of this UICP field demonstration was to evaluate the extent to which heat-treated microbial cultures can effectively seal undesired flow pathways. The ureolytic bacterium, *Sporosarcina pasteurii*, was the source of the urease enzyme in this study but cultures were briefly heat-treated prior to injection to inactivate the microbes while preserving enzyme activity. The use of heat-treated cells with intact enzyme activity may offer a viable alternative in situations where injection of live cells is problematic from either a logistical or regulatory standpoint. The heat treatment also mimics conditions in the deeper subsurface where elevated temperature would impact cell survival.

The field demonstration of UICP sealing in the presence of $CO_2$-affected brine was conducted in a 24.4 cm (9.625 inch) outer-diameter cased test well at the William Crawford Gorgas Electric Generating Plant (Alabama Power, Southern Company) near Parrish, Alabama, USA, hereafter referred to as “Gorgas”. The well was drilled to a depth of 1498 m by the U.S.

Department of Energy to assess the potential for geologic carbon sequestration. The target formation(s), however, proved to be unfavorable for $CO_2$ storage so the well has been used instead for research purposes. Previous field tests, which used live microbial cultures as the source of the urease enzyme, focused on sealing a hydraulic fracture in a sandstone formation 340 m (1115 ft) below ground surface (bgs) [16] and sealing a channel in the well cement 310 m (1017 ft) bgs [9]. Additional details about the well are available in Phillips *et al*. (2016)[16] and in Section 2.1 below.

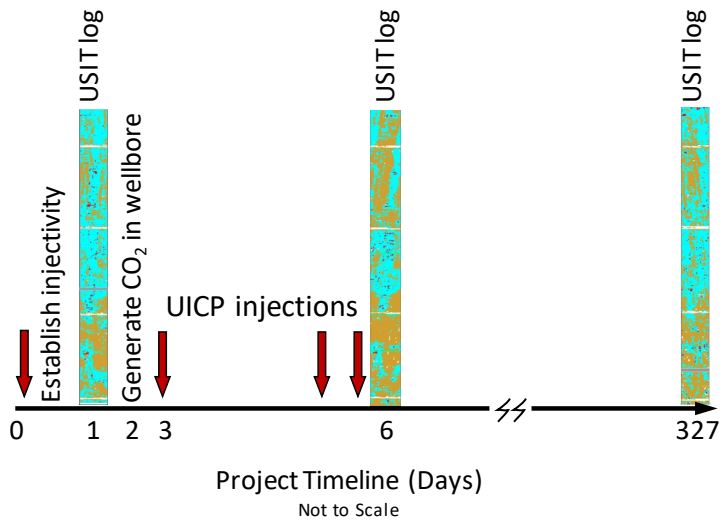


**Figure 1.** The experimental timeline of the field demonstration. Samples were collected from the downhole injection zone four times (red arrows). Injections of 5% HCl and $NaHCO_3$ were used to generate $CO_2$ in the wellbore annular defect. Ultrasonic imaging (USIT) logs were collected twice during the field demonstration (Day 1, 6) to image the materials in the wellbore annulus, before and after injections of UICP-promoting fluids. Biomineralization in the annular cement channel was monitored during UICP injections using pressure and flow rate measurements. A third USIT log was acquired 11 months after the field work ended (Day 327).

Figure 1 summarizes the types of activities performed and order of events during the current field demonstration. Detailed descriptions of each activity follow in later sections. Water samples were collected four times over the course of the study (red arrows) to characterize

downhole geochemical and microbiological conditions. (This data will be reported elsewhere by project collaborators.) Because flow behind the casing at the study depth, 310 m (1017 ft) bgs, had been effectively minimized with UICP during the second field demonstration [9], acid injections were used first to dissolve the calcium carbonate biomineral and establish a flow path in the wellbore cement annulus. Once a channel was formed, $CO_2$ was produced behind the casing and injections of UICP-promoting fluids began. Throughout injection, pressure and flow rate were monitored to assess changes in injectivity, defined here as the flow rate divided by the injection pressure. Injectivity serves as a proxy for permeability or transmissivity since flow path geometry through the compromised cement is unknown. Decreasing injectivity is an indication of mineral formation in the channel[15, 17-20]. In addition, ultrasonic imaging logs were conducted twice to assess the extent of mineral formation behind the casing due to UICP. The field demonstration was ended when the injection pump's maximum pressure and minimum flow rate were reached. A subsequent seal integrity check was performed approximately 11 months (327 days) after the field demonstration ended and additional ultrasonic well logging was performed. Following the seal integrity check, the well was plugged and abandoned in accordance with regulatory requirements.

## 2. Materials and Methods

### *2.1 Well preparation and experimental design*

The current work is the research team's third field demonstration of ureolysis-induced calcium carbonate precipitation in the Gorgas well. This field demonstration was conducted at 310 m (1017 ft) bgs, the same depth as the previous well cement sealing demonstration where the temperature is approximately 15°C. The static water level in the well was approximately 10 m (30 ft) bgs at the beginning of the demonstration. The three sidewall perforations in the steel casing drilled during the previous study at 310.0, 310.3, and 310.9 m (1017, 1018 and 1020 feet) bgs were again used to access the cement annulus [9]. The 7.3 cm (2-7/8-inch) steel

injection tubing string extended from the surface to a depth of 312.7 m (1026 ft) bgs, including a 1 m (3 ft) perforated pup joint ending in a collar stop at 311.6 m (1022 ft). A bull plug closed off the end of the tubing at 312.8 m (1026 ft) bgs. The target injection zone was isolated by a packer above the casing perforations and a bridge plug below. The packer was placed between the tubing string and casing at a depth of 296.6 m (973 ft) bgs. A 24.4 cm (9-5/8-inch) cast iron bridge plug was set at a depth of 316 m (1037 ft) bgs and was topped with 1.5 m (5 ft) of cement to prevent fluid from migrating down the casing below the injection point. An 11 L (2.9 gal) slickline dump bailer was used to deliver fluids to the subsurface. Fluids were pumped into the bailer at the wellhead with transfer pumps and hoses dedicated to each fluid type. The bottom of the bailer was fitted with a glass disk that shattered upon impact with the collar stop at the target injection zone. Fresh water pumped down the tubing string after impact flushed the fluids from the bailer, tubing string, and wellbore through the sidewall perforations and into the cement channel behind the casing. Bailer delivery downhole and return to the surface took approximately 20 minutes.

The initial injectivity [L/min*MPa (gal/min*psi)] of the system was obtained by monitoring the wellhead pressure during an initial injection test of water down the tubing string. Injectivity was low initially since the prior field demonstration [9] had sealed the flow channel behind the casing in the same injection zone.

After the initial injection test, 3 bailers (33 L) of 5% HCl were delivered downhole to expand the flow path in the cement by dissolving biomineral formed during the previous field demonstration in the well. Following the expansion of a flow path in the cement, three bailers (33L) each of 5% HCl and 100 g/L $NaHCO_3$ were injected in an alternating fashion to produce $CO_2$ in the near wellbore environment according to Eqn. 2.

$$HCl + NaHCO_3 \rightarrow Na^+ + Cl^- + H_2O + CO_2(g) \qquad \text{Eqn. 2}$$

Direct $CO_2$ injection would have required a rigorous EPA Class VI injection permitting review process, which was not feasible during the timeframe of this project. The amount of HCl (1.26 kg or 34.8 mol) and $NaHCO_3$ (3.3 kg or 39.2 mol) injected for $CO_2$ production have a theoretical $CO_2$ production of approximately 35 mol, assuming that all the reactants were consumed in the intended reaction. The HCl injections to open a flow path in the wellbore annulus could have produced additional $CO_2$, depending on the extent of the reaction with calcium carbonate produced during the previous field demonstration.

Following $CO_2$ production, injections of UICP-promoting fluids began. For the first 2 days of injecting UICP-promoting fluids, one bailer of heat-treated cells was followed by two bailers of urea – calcium solution. Starting the end of the second day, the bailer contents alternated between heat-treated cells and urea – calcium solution.

### *2.2 Well characterization – USIT logs and sampling*

An ultrasonic imaging (USIT) log was collected twice during the field demonstration using an Isolation Scanner (Schlumberger) which produces a Solid-Liquid-Gas (SLG) map of the wellbore annulus via measurement of the cement impedance and flexural wave attenuation. The first USIT log was recorded after establishing a flow path with acid injection but before $CO_2$ production. The second USIT log was collected at the end of the field demonstration after 4 days of injecting UICP-promoting fluids. Another USIT log was acquired approximately 11 months (327 days) after the end of the field demonstration prior to plugging and abandoning the Gorgas well. Image analysis using ImageJ software (v1.8.0_172) was performed to quantify the solids detected behind the casing in each USIT log. The area of the image occupied by tan pixels, which represent solids, were measured after applying a color threshold to the image histogram. Solids correspond to hue values between 17 – 50 on the 0 – 255 scale. The full 0 – 255 range was applied for both saturation and brightness.

At the end of the field demonstration, samples of precipitates were scraped from the injection tubing and 'sludge' from the well sump and bottom plug was collected for analysis. These samples were subjected to X-ray diffraction (XRD) analysis to characterize the mineral composition. Samples were dried and pulverized then deposited onto a glass slide coated with a thin layer of petroleum jelly and analyzed with a Scintag X1 Powder X-ray diffractometer equipped with a copper (Cu) k-alpha X-ray source housed at the Imaging and Chemical Analysis Laboratory (ICAL) at Montana State University.

## 2.3 *UICP-promoting fluids*

Microbial cultures were started by inoculating 1L 18.5 g/L BHI media (Becton Dickinson, Franklin Lakes, NJ) plus 20 g/L urea (Fisher Scientific) with 10 mL (4.4 x $10^6$ CFU/mL) of frozen stock of *Sporosarcina pasteurii* (ATCC® 11859™). After approximately 16 hours, the 1L culture was transferred to 45.4 L (12 gal) yeast extract medium (15.5 g/L yeast extract, 24 g/L urea (Dyno Nobel, Inc, Deer Island OR), 1 g/L $NH_4Cl$). The 45.4 L cultures were grown at 30°C for approximately 24 hours in 56.8-L (15-gal) conical bottom reactors equipped with aeration, temperature control, ventilation, and recirculation as described in Kirkland *et al*. (2020) [7] and shown in Figure 2.

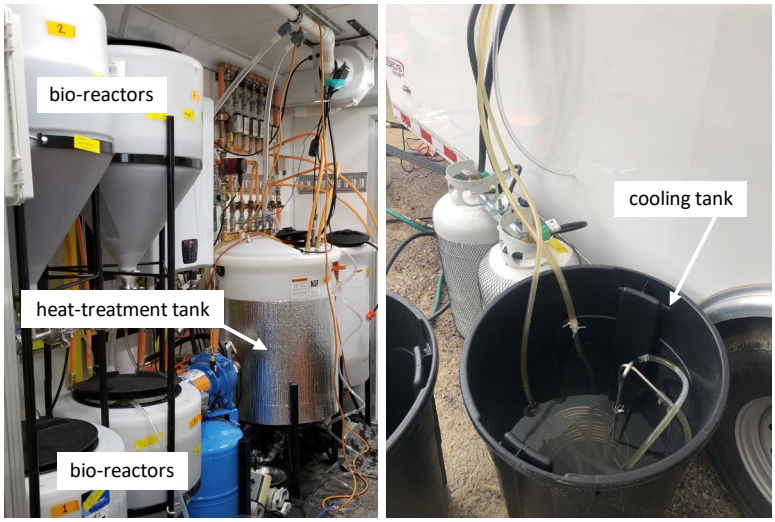

221 **Figure 2.** Heat-treatment system developed in the custom MSU mobile laboratory received flow
222 from 24-hr cultures grown in the bioreactors (left). The 60°C heat-treatment tank (left) was
223 wrapped in insulation to reduce heat losses. The cooling tank, located outside of the trailer,
224 contained water below 30°C. Cultures were pumped through stainless steel coils in both the
225 heating and cooling tanks.
226

227 After approximately 24 hours of growth in the conical bottom reactors, the *S. pasteurii*
228 cultures were combined in a holding tank from which they were pumped with a peristaltic pump
229 into the heat-treatment system (Figure 2). Microbes were heat-treated as they flowed through
230 coiled tubing suspended in reactor heated to 60°C. During the first two days of the field
231 demonstration, a 15.24 m (50-ft), 1.27 cm (1/2-inch) OD 316 stainless steel (SS) coil was used.
232 For the remainder of the experiment, a second coil was added in series (15.24 m (50-ft), 0.95
233 cm (3/8-inch) OD 316 SS) to allow for higher flowrates while maintaining adequate residence
234 time in the 60°C reactor (i.e. 8-13 minutes). Temperature was maintained at 60°C in the hot
235 water bath with immersion heaters and insulation was wrapped around the tank to reduce heat
236 loss. Heat-treated cells were cooled using a 15.24 m (50-ft), 0.95 cm (3/8-inch) OD 316 SS coil
237 submerged in a < 30°C water bath to protect the urease enzyme from inactivation due to
238 prolonged exposure to elevated temperature (Figure 2) [21]. Cooled cultures were stored in a
239 holding tank at ambient temperature until they were delivered into the well.

240 Microbial cultures were sampled each day before and after heat treatment. Population
241 analysis was performed using the drop plate method [22] to count colony forming units (CFU).
242 The detection limit was 1 x $10^3$ CFU/mL. Before filling the bailer for an injection, the heat-
243 treated cultures were also sampled for pH, electrical conductivity (EC), urea analysis with the
244 Jung Assay [23], and optical density. Optical density ($OD_{600}$) was measured in triplicate to monitor
245 growth in the reactors from 200 µL samples in a 96-well plate at 600 nm using an Infinite F50
246 plate reader (Tecan, Switzerland). $OD_{600}$ of the fresh YE medium blank was 0.05 ± 0.002.

Urea-calcium solution (U+C) was prepared daily with 72 g/L urea and 124 g/L $CaCl_2$ (Peladow, Occidental Chemical Corp., Dallas, TX) in a 132-L (35-gal) tank. The U+C solution was mixed with a drill-powered mixer and sampled for pH, urea, and $Ca^{2+}$ analyses.

### *2.4 Batch studies – Ureolytic activity*

The ureolytic activity of heat-treated cultures was compared to that of actively growing microbial cultures using EC [mS/cm] measurements. Due to the production of $NH_4^+$ ions during ureolysis (Eqn. 1), increases in EC over time can be used as a proxy to compare ureolysis rates between samples [24]. Ten mL of 20 g/L urea (Fisher Scientific) solution was added to 10 mL samples of both actively growing *S. pasteurii* cultures and heat-treated cultures in 50 mL conical tubes. Mixtures were vortexed initially and immediately prior to EC measurements. EC measurements were performed every 30 minutes for 3 hours.

## *3.* **Results**

### *3.1 Reduced Injectivity*

Wellhead pressure and pumping flow rate were monitored and recorded as water was injected to push each bailer of fluids into the wellbore channel. Figure 3 shows the injectivity of each bailer delivery as a function of total injection volume. Approximately 242 L (64 gal) of heat-treated microbial cultures (22 bailers) and 329 L (87 gal) of U+C media (30 bailers) were injected over 4 days. The UICP treatment resulted in an order-of-magnitude reduction of injectivity in the channel (Figure 3) which is indicative of biomineral formation in flow pathways outside the well casing. The preliminary low injectivity of 0.76 L/min*MPa ($1.38 \times 10^{-4}$ gpm/psi) measured during initial freshwater injection increased to 9.33 L/min*MPa ($1.73 \times 10^{-3}$ gpm/psi) after the injection of HCl to open a flow path (Figure 3). The highest injectivity during the experiment occurred during the injection of HCl and $NaHCO_3$ to produce $CO_2$ when the flow rate was 8.33 L/min (2.2 gpm) at 0.49 MPa (708 psi) for an injectivity of 17.1 L/min*MPa ($3.11 \times 10^{-3}$

gpm/psi). After $CO_2$ production but before UICP treatment, the channel conveyed 4.9 L/min at 0.49 MPa (1.3 gpm at 712 psi), for an injectivity of 10.0 L/min*MPa ($1.83 \times 10^{-3}$ gpm/psi). During UICP treatment, injectivity was stable for two days before decreasing rapidly. On the third day after beginning UICP injections and at a cumulative injection volume of approximately 1740 L (460 gal), injectivity decreased significantly before leveling off, then decreasing again in a 'stair-step' pattern (Figure 3). The final flow-pressure relationship at the end of the field demonstration were 0.757 L/min at 0.761 MPa (0.2 gpm at 1104 psi) which equates to an injectivity of 0.99 L/min*MPa ($1.81 \times 10^{-4}$ gpm/psi). An injection test 11 months later produced an injectivity of 2.56 L/min*MPa ($4.67 \times 10^{-4}$ gpm/psi) which increased to 8.62 L/min*MPa ($1.57 \times 10^{-3}$ gpm/psi) following sustained pumping. Red arrows in Figure 3 indicate when USIT logs were acquired.

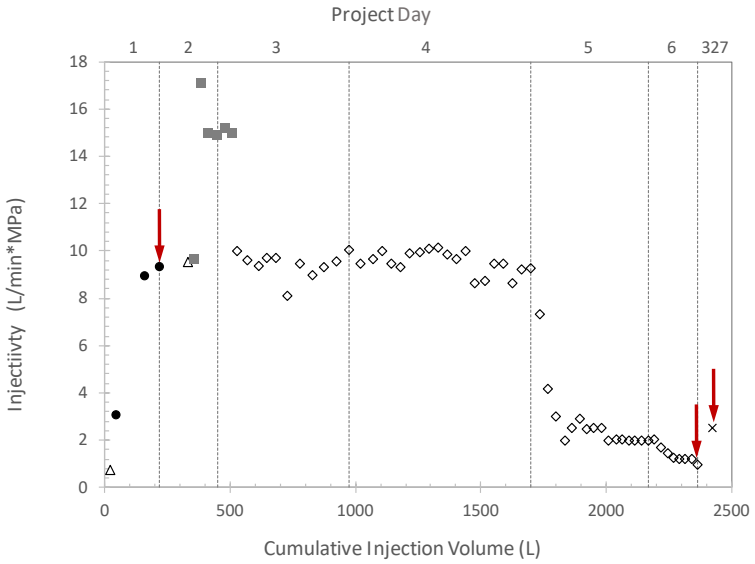


**Figure 3.** Injections of 5% HCl were used to open a flow path behind the well casing and then injections of 5% HCl and $NaHCO_3$ were used to generate $CO_2$ in the annular cement channel. Subsequent injections of UICP-promoting fluids reduced the injectivity by an order-of-magnitude

over days 3-6. Fresh water injections (Δ), 5% HCl injections (•), HCl/$NaHCO_3$ injections to produce $CO_2$ (■), UICP-promoting injections (◊), and pre-abandonment injection test (x). Red arrows indicate USIT logs. Vertical lines indicate days along secondary x-axis; time scale is not linear.

### *3.2 USIT logs*

The Gorgas well was logged ultrasonically twice during the field demonstration and again 11 months later (Figure 3, red arrows). USIT logs (Figure 4) show a 2D projection of the materials detected immediately behind the casing (right panel of each log) as a function of depth in the borehole (left panel of each log). In the first USIT log acquired during the current field work (left), the acid treatment appears to have expanded a channel outside the casing (black oval) relative to the final USIT log recorded at the end of the prior wellbore sealing demonstration[9]. The corresponding injectivity was 9.33 L/min*MPa ($1.70 \times 10^{-3}$ gpm/psi) (Figure 3). After UICP treatment in the presence of $CO_2$-affected brine (middle), there was a noticeable increase in the presence of solids in the channel in the region of the side wall perforations 300 – 310 m (990-1019 ft) bgs and more than 30 m (100 ft) above the injection point (red ovals). Compared to the initial USIT log, the post-UICP log shows a 58% increase in the image area occupied by solids behind the casing for the depth interval shown in Figure 4. The USIT log recorded on Day 327, approximately 11 months after the end of the field work (Figure 4, right) prior to plugging and abandoning the well, shows that significant solids remain despite the loss of solids relative to the Post-UICP log. The image area occupied by solids measured in this last USIT log is 30% greater than in the initial USIT log. The relative abundance of solids in the well-log images is consistent with injectivity values recorded over the course of the fieldwork. Higher proportions of solids correspond to lower injectivity and vice versa.

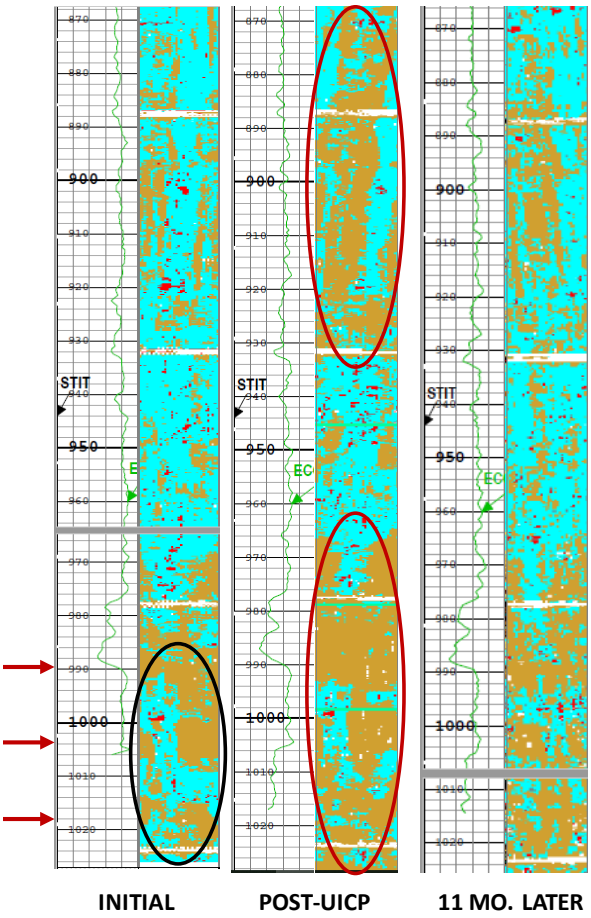


**Figure 4.** USIT logs showing a 2D projection of the materials immediately outside the casing before and after UICP treatment, where tan=solids, blue=liquid and red=gas detected. Fluids were able to access the cement defect/channel in three potential locations (990, 1004, 1017-1019 feet below ground surface) indicated by red arrows due to previously drilled sidewall perforations. Before production of $CO_2$ and UICP treatment, a channel was observed in the solid material detected behind the casing (black oval on left panel). After UICP treatment a significant increase in the amount of solid was observed (red ovals, middle panel). A follow-up USIT log 11 months later (Day 327, right panel) shows that significant solids remained in the location despite some loss.

### *3.3 Sample analysis*

XRD analysis of mineral samples collected from the injection tubing show that the mineral was 74.9% calcite ($CaCO_3$), 22.2% vaterite ($CaCO_3$), and 2.9% quartz ($SiO_2$). A sample from the well sump, which is located between the collar stop and the bottom plug, was 67.2% quartz and

331 32.8% magnetite ($Fe_3O_4$). Two samples of solids collected from the bottom plug were
332 predominantly iron species, magnetite and iron (III) oxide hydroxide (FeO(OH)), with quartz
333 comprising 33% and 25% of each sample, respectively.
334
335 *3.4 Heat treatment of microbial cultures*
336 *Sporosarcina pasteurii* cultures were grown to an average concentration of $2.5 \times 10^8$ CFU/mL
337 in the mobile laboratory conical bottom bio-reactors prior to heat-treatment. No colonies of
338 heat-treated cells were observed above the detection limit on the agar plates after 24 hours.
339 Batch studies to compare the ureolytic activity of growing vs. heat-treated cultures showed
340 larger increases in EC in the heat-treated cultures than in the growing cultures. EC increased
341 on average 41% more in heat-treated samples, with a standard deviation of 23 percentage
342 points. Excluding Day 2 data, which was an outlier, EC increased 51% more in heat-treated
343 cultures (St.dev = 7 percentage points).
344
345 **4. Discussion**
346 Presence of $CO_2$ in the wellbore annulus does not appear to have impeded calcium
347 carbonate mineral formation as evidenced by the order-of-magnitude reduction in injectivity and
348 the increased solids detected in the post-UICP treatment USIT log. These findings corroborate
349 previous studies which have found that UICP can occur in the presence of $CO_2$[25, 26].The 'stair
350 step' behavior of injectivity reduction is characteristic of UICP sealing in channels or fractures,
351 where substantial mineral precipitation is often necessary before measurable flow restriction
352 occurs. In these channel-type systems, mineral formation must reach a critical threshold before
353 the ratio of pressure and flow measurements, or injectivity, registers significant change. Once
354 the flow path is partially restricted, however, conditions are favorable at that location for
355 additional mineral to form and injectivity decreases dramatically over a relatively short time
356 frame [15]. In this field demonstration, this pattern appears to repeat three times (Figure 3), with

357 the decreases occurring the morning of the third day of injecting UICP-promoting fluids (at a
358 cumulative injection volume of approximately 1741 L (460 gal)), the morning of the fourth day
359 (approximately 2214 L (585 gal)) and at the final bailer injection (2362 L (624 gal)). Similar
360 behavior has been observed in other studies monitoring sealing of channels with UICP [15, 16, 18-20,
361 27, 28] though some report only a single 'stair step' before the channel sealed. The results
362 obtained during this field demonstration suggest that when a preferred flow path sealed due to
363 UICP, the reactants were re-routed through another path in the wellbore annulus until that one
364 also sealed, and so on. This sealing behavior is in contrast to that reported where the seal
365 formed within a higher permeability sandstone rock matrix in a waterflood injection well [7, 8] or
366 within a laboratory bio-reactor sand pack [29]. In these cases, mineralization and sealing of the
367 pore spaces proceeded gradually over time in a nearly linear fashion. In systems where
368 permeability is more evenly distributed, each pore that fills or is blocked with bio-mineral
369 fractionally reduces the injectivity of the system until few pathways remain open[30].
370 The XRD data from the tubing string samples confirms that calcium carbonate precipitation
371 occurred downhole following the injection of UICP-promoting fluids. The fact that calcium
372 carbonate polymorphs were not detected in the sump and bottom plug suggests that the
373 mineralizing fluids were successfully transported out of the wellbore and that the precipitation
374 reactions proceeded within the cement channel as intended. The presence of iron species in
375 the well sump and bottom plug is to be expected. Raising and lowering the bailer repeatedly
376 within the steel tubing string, injection of acid to open a flow path, and injection of acid and
377 $NaHCO_3$ to form $CO_2$ likely contributed to the accumulation of iron species at the bottom of the
378 tubing string.
379 Extended exposure to elevated temperatures (greater than 65°C) is known to inactivate the
380 urease enzyme which could inhibit ureolysis-induced mineral precipitation [21, 31]. In this study,
381 however, EC data points to higher rates of ureolysis in the heat-treated cultures. This apparent
382 contradiction is related to the temperature, 60°C, and duration of exposure the microbial

383 cultures experienced which was limited to 8 – 13 minutes. The goal was to inactivate the cell
384 without inactivating the enzyme. Thus, one explanation for the observed increase in ureolytic
385 activity in heat-treated cultures relates to the integrity of the cell wall following heat stress. A
386 partial breakdown of bacterial cell walls could enhance transport of urea into or urease enzyme
387 out of the cell, thereby increasing urea hydrolysis rates. In the case of the live cells, transport of
388 urea into the cells (or urease out of the cells) is recognized as a rate-limiting step in urea
389 hydrolysis [32, 33].

390 The USIT logs acquired during this project show both the potential of the UICP
391 biotechnology to seal leakage pathways in wellbores as well as some remaining questions
392 related to seal durability. The Post-UICP USIT log shows extensive solids precipitation not only
393 in the immediate vicinity of the injection, but also far above. Due to the presence of a bridge
394 plug in the casing, it was not possible to observe the extent of mineral formation below the
395 injection point though there is no reason to assume mineral could not have formed there.

396 The available data regarding the durability of UICP mineral seals in this well is mixed and
397 highlights the need for additional research on the topic. First, the preliminary water injection,
398 shown as the first data point in Figure 3, yielded a low initial injectivity of 0.76 L/min*MPa
399 ($1.38 \times 10^{-4}$ gpm/psi) and indicates that the seal produced during the previous demonstration of
400 UICP in the well [9] remained in place during the 18 months between field demonstrations.
401 Moreover, our small business team members have successfully deployed UICP to seal leakage
402 pathways in 11 commercial oil and gas wells in Colorado and Wyoming [7] with no additional
403 treatment required to satisfy regulatory standards for operation or abandonment. Four of these
404 wells in the Denver-Julesburg Basin of Colorado were horizontal production wells in the
405 Niobrara formation experiencing sustained casing pressure ranging from 80 psi (0.55 MPa) to
406 899 psi (6.2 MPa) prior to UICP treatment. Immediately after treatment, casing pressure in all
407 wells was reduced to 0 psi (0 MPa). After six months in operation following UICP treatment, two
408 of the wells produced casing pressure readings of 5 psi (0.03 MPa) and 2 psi (0.01 MPa)

409 (unpublished data), which is well below the regulatory value of 50 psi (0.34 MPa) that triggers
410 remedial action. The remaining two wells, which had initially yielded the highest sustained
411 casing pressures of 395 psi (2.7 MPa) and 899 psi (6.2 MPa), remained at 0 psi (unpublished
412 data). These findings from the Gorgas well and commercial production wells provide evidence
413 that the calcium carbonate biomineral seal can be durable over a timeframe of months to years.
414 At the same time, the USIT log acquired prior to abandoning the well (Figure 4, right) shows
415 a loss of solids relative to the Post-UICP USIT log acquired at the end of the field demonstration
416 (Figure 4, middle). Injectivity data suggests that the seal was further compromised following
417 sustained pumping during the subsequent injection test. There are several possible
418 explanations for this observed behavior. First, residual $CO_2$ in the near wellbore environment
419 may have produced low-pH conditions favorable for calcium carbonate dissolution. Second,
420 heat-treatment of cells may have altered the microbial phenotype such that cells did not firmly
421 attach to surfaces as a biofilm prior to mineralizing. It is not possible, given the available data
422 from this field demonstration, to say with certainty which of these scenarios, if either, caused the
423 loss of solids after the field demonstration ended. Two points, however, are worth noting.
424 First, acidic pH conditions (e.g. < pH 7) are known to promote calcium carbonate dissolution
425 wherein the rate of dissolution depends on complex geochemical and hydrodynamic factors
426 related to fluid saturation states at the solid-liquid interface[25]. The surface area of the mineral
427 seal exposed to wellbore fluid is of critical importance. We hypothesize that the amount of
428 calcium carbonate that dissolves due to low pH conditions is proportional to the exposed
429 surface area. Therefore, the seal in Figure 4, which has flow pathways around the well
430 circumference and exposed surface area distributed over several meters along the wellbore
431 axis, would be expected to be impacted more by acidic conditions than a similar aperture seal
432 with fewer flow paths and less exposed surface area. The relatively uniform dissolution of
433 exposed seal edges, apparent in the two USIT logs, should be noted.

Second, despite exhibiting higher ureolysis rates than live cells, the heat-treated *S. pasteurii* cultures do not appear to have produced as robust a seal as live cells have done in previous demonstrations [9]. Ma *et al.* [34] indicate that intact cell structure promotes nucleation of mineral during UICP. Secchi *et al.* [35] found preferential attachment of elongated, motile cells (like *S.pasteurii*) on the downstream side of surface roughness under moderate hydrodynamic conditions. Heat-treatment would be expected to modify both of these phenotypic characteristics – cell shape and motility – via damage to the cell membrane, thereby decreasing the capture efficiency or attachment of cells to the surfaces in the wellbore and by reducing the potential of the cell to act as a nucleation site. Heat-treated cells would be more likely to behave instead as passive particles in the flow where they would be intercepted by surfaces on the upstream side of wellbore annulus surface roughness [35]. This 'passive particle' behavior may be useful in explaining the formation of mineral so far above the injection zone. Heat-treated cells may have been carried in the flow up the well casing beyond the injection point until they intercepted a surface due, in part, to cell lysis and other phenotypic changes.

Further numerical simulations [36, 37] and validation of these hypotheses in the lab could elucidate the mechanisms that promote a durable seal and advance the process to develop deployable microbial cultures for large-scale adoption of the biotechnology in the field [38].

## 5. Conclusions

The presence of $CO_2$ did not impede mineral formation during the field demonstration as evidenced by the reduction in injectivity observed during UICP treatment as well as the additional solids present in the post-treatment USIT log. Additionally, urease enzyme from heat-treated microbial cultures was an effective catalyst for the UICP reactions and higher ureolysis rates were observed in the heat-treated cultures than in live cultures, perhaps due to cell lysis. At the same time, the seal formed in the wellbore annulus in this field demonstration was less robust than a previous seal produced by UICP in the same well without the presence of $CO_2$-

affected brine and using live microbes. The results of this experiment suggest that UICP can be promoted in the presence of $CO_2$ impacted brine to seal leakage pathways and may be effective to ensure storage of $CO_2$ in geologic carbon sequestration scenarios. Further research is needed to study the durability of the seal over extended time scales under adverse wellbore conditions.

**Acknowledgements**

This material is based upon work supported by the Department of Energy under Grant No. DE-FE0024296. Any opinions, findings, conclusions or recommendations expressed herein are those of the authors and do not necessarily reflect the views of the Department of Energy (DOE). This work was performed in part at the Montana Nanotechnology Facility (MONT), a member of the National Nanotechnology Coordinated Infrastructure (NNCI), which is supported by the National Science Foundation (Grant# ECCS-1542210). The authors thank Abby Thane Davis and Laura Dobeck at the Center for Biofilm Engineering, as well as Nathaniel Rieders at ICAL.

**References**

1. Tong, D.; Zhang, Q.; Zheng, Y.; Caldeira, K.; Shearer, C.; Hong, C.; Qin, Y.; Davis, S. J., Committed emissions from existing energy infrastructure jeopardize 1.5 °C climate target. *Nature* **2019,** *572* (7769), 373-377.
2. Agency, I. E., The Role of CO2 Storage. IEA: Paris, 2019; Vol. Exploring Clean Energy Pathways.
3. Jafariesfad, N.; Sangesland, S.; Gawel, K.; Torsæter, M., New Materials and Technologies for Life-Lasting Cement Sheath: A Review of Recent Advances. *SPE Drilling & Completion* **2020,** *35* (02), 262-278.
4. Todorovic, J.; Raphaug, M.; Lindeberg, E.; Vralstad, T.; Buddensiek, M. L., Remediation of Leakage through Annular Cement Using a Polymer Resin: a Laboratory Study. *8th Trondheim Conference on Co2 Capture, Transport and Storage* **2016,** *86*, 442-449.
5. Genedy, M.; Kandil, U. F.; Matteo, E. N.; Stormont, J.; Taha, M. M. R., A new polymer nanocomposite repair material for restoring wellboreseal integrity. *International Journal of Greenhouse Gas Control* **2017,** *58*, 290-298.
6. Genedy, M.; Matteo, E. N.; Stenko, M.; Stormont, J. C.; Taha, M. R., Nanomodified Methyl Methacrylate Polymer for Sealing of Microscale Defects in Wellbore Systems. *J. Mater. Civ. Eng.* **2019,** *31* (7).

7. Kirkland, C. M.; Hiebert, R.; Hyatt, R.; McCloskey, J.; Kirksey, J.; Thane, A.; Cunningham, A. B.; Gerlach, R.; Spangler, L.; Phillips, A. J., Direct Injection of Biomineralizing Agents to Restore Injectivity and Wellbore Integrity. *SPE Production & Operations* **2020,** *Preprint* (Preprint), 8.
8. Kirkland, C. M.; Thane, A.; Hiebert, R.; Hyatt, R.; Kirksey, J.; Cunningham, A. B.; Gerlach, R.; Spangler, L.; Phillips, A. J., Addressing wellbore integrity and thief zone permeability using microbially-induced calcium carbonate precipitation (MICP): A field demonstration. *Journal of Petroleum Science and Engineering* **2020,** *190*, 107060.
9. Phillips, A. J.; Troyer, E.; Hiebert, R.; Kirkland, C. M.; Gerlach, R.; Cunningham, A.; Spangler, L.; Kirksey, J.; Rowe, W.; Esposito, R., Enhancing wellbore cement integrity with microbially induced calcite precipitation (MICP): a field scale demonstration. *Journal of Petroleum Science and Engineering* **2018,** *171*, 1141-1148.
10. Fujita, Y.; Ferris, E. G.; Lawson, R. D.; Colwell, F. S.; Smith, R. W., Calcium carbonate precipitation by ureolytic subsurface bacteria. *Geomicrobiol. J.* **2000,** *17* (4), 305-318.
11. Krajewska, B., Ureases I. Functional, catalytic and kinetic properties: A review. *Journal of Molecular Catalysis B-Enzymatic* **2009,** *59* (1-3), 9-21.
12. Oppenheimer-Shaanan, Y.; Sibony-Nevo, O.; Bloom-Ackermann, Z.; Suissa, R.; Steinberg, N.; Kartvelishvily, E.; Brumfeld, V.; Kolodkin-Gal, I., Spatio-temporal assembly of functional mineral scaffolds within microbial biofilms. *Npj Biofilms and Microbiomes* **2016,** *2*.
13. Stocks-Fischer, S.; Galinat, J. K.; Bang, S. S., Microbiological precipitation of CaCO3. *Soil Biol. Biochem.* **1999,** *31* (11), 1563-1571.
14. Zambare, N. M.; Naser, N. Y.; Gerlach, R.; Chang, C. B., Mineralogy of microbially induced calcium carbonate precipitates formed using single cell drop-based microfluidics. *Scientific Reports* **2020,** *10* (1), 17535.
15. Kirkland, C. M.; Norton, D.; Thane, A.; Hiebert, R.; Hommel, J.; Kirksey, J.; Esposito, R.; Cunningham, A.; Gerlach, R.; Spangler, L.; Phillips, A. In *Biomineralization and wellbore integrity: a microscopic solution to subsurface fluid migration*, 14th Greenhouse Gas Control Technologies Conference, Melbourne, Australia, 21-26 October 2018; Melbourne, Australia, 2019.
16. Phillips, A. J.; Cunningham, A. B.; Gerlach, R.; Hiebert, R.; Hwang, C.; Lomans, B. P.; Westrich, J.; Mantilla, C.; Kirksey, J.; Esposito, R.; Spangler, L., Fracture Sealing with Microbially-Induced Calcium Carbonate Precipitation: A Field Study. *Environ. Sci. Technol.* **2016,** *50* (7), 4111-4117.
17. Cuthbert, M. O.; McMillan, L. A.; Handley-Sidhu, S.; Riley, M. S.; Tobler, D. J.; Phoenix, V. R., A Field and Modeling Study of Fractured Rock Permeability Reduction Using Microbially Induced Calcite Precipitation. *Environ. Sci. Technol.* **2013,** *47* (23), 13637-13643.
18. Minto, J. M.; MacLachlan, E.; El Mountassir, G.; Lunn, R. J., Rock fracture grouting with microbially induced carbonate precipitation. *Water Resour. Res.* **2016,** *52* (11), 8810-8827.
19. Tobler, D. J.; Minto, J. M.; El Mountassir, G.; Lunn, R. J.; Phoenix, V. R., Microscale Analysis of Fractured Rock Sealed With Microbially Induced CaCO3 Precipitation: Influence on Hydraulic and Mechanical Performance. *Water Resour. Res.* **2018,** *54* (10), 8295-8308.
20. Kirkland, C. M.; Norton, D.; Firth, O.; Eldring, J.; Cunningham, A. B.; Gerlach, R.; Phillips, A. J., Visualizing MICP with X-ray uCT to enhance cement defect sealing. *International Journal of Greenhouse Gas Control* **2019,** *86*, 93 - 100
21. Feder, M. J.; Akyel, A.; Morasko, V. J.; Gerlach, R.; Phillips, A. J., Temperature-dependent inactivation and catalysis rates of plant-based ureases for engineered biomineralization. *Engineering Reports* **2020,** *n/a* (n/a), e12299.
22. Herigstad, B.; Hamilton, M.; Heersink, J., How to optimize the drop plate method for enumerating bacteria. *J. Microbiol. Methods* **2001,** *44* (2), 121-129.
23. Jung, D.; Biggs, H.; Erikson, J.; Ledyard, P. U., New colorimetric reaction for endpoint, continuous-flow and kinetic measurement of urea *Clin. Chem.* **1975,** *21* (8), 1136-1140.

24. Shashank, B. S.; Minto, J. M.; Singh, D. N.; El Mountassir, G.; Knapp, C. W., Guidance for Investigating Calcite Precipitation by Urea Hydrolysis for Geomaterials. *J. Test. Eval.* **2018,** *46* (4), 1527-1538.
25. Mitchell, A. C.; Phillips, A.; Schultz, L.; Parks, S.; Spangler, L.; Cunningham, A. B.; Gerlach, R., Microbial CaCO3 mineral formation and stability in an experimentally simulated high pressure saline aquifer with supercritical CO2. *International Journal of Greenhouse Gas Control* **2013,** *15*, 86-96.
26. Verba, C.; Thurber, A. R.; Alleau, Y.; Koley, D.; Colwell, F.; Torres, M. E., Mineral changes in cement-sandstone matrices induced by biocementation. *International Journal of Greenhouse Gas Control* **2016,** *49*, 312-322.
27. Phillips, A. J.; Eldring, J.; Hiebert, R.; Lauchnor, E.; Mitchell, A. C.; Cunningham, A.; Spangler, L.; Gerlach, R., Design of a meso-scale high pressure vessel for the laboratory examination of biogeochemical subsurface processes. *Journal of Petroleum Science and Engineering* **2015,** *126*, 55-62.
28. Phillips, A. J.; Lauchnor, E.; Eldring, J.; Esposito, R.; Mitchell, A. C.; Gerlach, R.; Cunningham, A. B.; Spangler, L. H., Potential CO2 Leakage Reduction through Biofilm-Induced Calcium Carbonate Precipitation. *Environ. Sci. Technol.* **2013,** *47* (1), 142-149.
29. Kirkland, C. M.; Zanetti, S.; Grunewald, E.; Walsh, D. O.; Codd, S. L.; Phillips, A. J., Detecting Microbially Induced Calcite Precipitation in a Model Well-Bore Using Downhole Low-Field NMR. *Environ. Sci. Technol.* **2017,** *51* (3), 1537-1543.
30. Ferris, F. G.; Stehmeier, L. G.; Kantzas, A.; Mourits, F. M., Bacteriogenic mineral plugging. *J. Can. Pet. Technol.* **1996,** *35* (8), 56-61.
31. Illeova, V.; Polakovic, M.; Stefuca, V.; Acai, P.; Juma, M., Experimental modelling of thermal inactivation of urease. *J. Biotechnol.* **2003,** *105* (3), 235-243.
32. Beckers, G.; Bendt, A. K.; Krämer, R.; Burkovski, A., Molecular identification of the urea uptake system and transcriptional analysis of urea transporter- and urease-encoding genes in Corynebacterium glutamicum. *J. Bacteriol.* **2004,** *186* (22), 7645-7652.
33. Mobley, H. L.; Island, M. D.; Hausinger, R. P., Molecular biology of microbial ureases. *Microbiological Reviews* **1995,** *59* (3), 451-480.
34. Ma, L.; Pang, A.-P.; Luo, Y.; Lu, X.; Lin, F., Beneficial factors for biomineralization by ureolytic bacterium Sporosarcina pasteurii. *Microbial Cell Factories* **2020,** *19* (1), 12.
35. Secchi, E.; Vitale, A.; Mino, G. L.; Kantsler, V.; Eberl, L.; Rusconi, R.; Stocker, R., The effect of flow on swimming bacteria controls the initial colonization of curved surfaces. *Nature Communications* **2020,** *11* (1).
36. Hommel, J.; Akyel, A.; Frieling, Z.; Phillips, A. J.; Gerlach, R.; Cunningham, A. B.; Class, H., A Numerical Model for Enzymatically Induced Calcium Carbonate Precipitation. *Applied Sciences* **2020,** *10* (13).
37. Cunningham, A. B.; Class, H.; Ebigbo, A.; Gerlach, R.; Phillips, A. J.; Hommel, J., Field-scale modeling of microbially induced calcite precipitation. *Computational Geosciences* **2019,** *23* (2), 399-414.
38. Landa Marbán, D.; Tveit, S.; Kumar, K.; Gasda, S., *Practical approaches to study microbially induced calcite precipitation at the field scale*. 2020.